DOI: https://doi.org/10.1016/j.jms.2021.111444

# Rotational Spectrum and Quantum Chemical Calculations of Methyl Cyanoacetate: A Compound of Potential Astrochemical Interest

Carolyn Gregory, Weslley G. D. P. Silva and Jennifer van Wijngaarden*

Department of Chemistry, University of Manitoba, Winnipeg, Manitoba, R3T 2N2, Canada

*Corresponding author

Email: vanwijng@cc.umanitoba.ca

Phone: (204)474-8379

Fax: (204)474-7608

*Abstract*

The rotational spectrum of methyl cyanoacetate ($H_3CO(CO)CH_2CN$) was investigated for the first time using Fourier transform microwave spectroscopy in the 6-19 GHz range. The observed spectral pattern is that of a single, dominant conformer and reveals both $^{14}N$ quadrupole hyperfine structure and characteristic A/E splittings due to the methyl internal rotor. The rotational constants determined from analysis of the complex spectral pattern confirm that the observed spectrum is that of the lowest energy conformer of methyl cyanoacetate predicted at the B3LYP-D3(BJ) and MP2 levels of theory using the aug-cc-pVTZ basis set. This global minimum corresponds to a geometry which orients the C-O-C=O and C-C-C=O dihedral angles in *syn* and *near anti* arrangements, respectively and is governed by a balance of stabilizing orbital interactions and destabilizing steric effects identified using non-covalent interaction and natural bond orbital analyses.

*Introduction*

With ongoing technical advances in the field of observational astronomy such as the commissioning of the Atacama Large Millimeter/Submillimeter Array (ALMA), there is an urgent need for laboratory-based spectroscopic studies of compounds of astrochemical interest to facilitate future detections in the interstellar medium (ISM). Of particular interest is the precise characterization of rotational energy states of potential candidates including the spectroscopic signatures of their conformers, minor isotopologues and excited vibrational states. For example, following the first detection of methyl acetate ($H_3CO(CO)CH_3$) [1] in Orion in 2013, increased attention turned to extending the experimental description of the energy states of this two methyl top system [2] and to predictions of spectroscopic parameters for deuterium substituted analogs [3]. Based on the prevalence of cyano-containing compounds in astronomy catalogs [4] of known interstellar and circumstellar species, methyl cyanoacetate ($H_3CO(CO)CH_2CN$) (MCA) is an excellent candidate for future astronomical searches.

There are no prior experimental studies of the rotational energy levels of MCA in any spectral region but a survey of the literature reveals interesting observations regarding the geometries and relative energies of the stable conformers. The vibrational spectrum has been the subject of several studies including reports in the gas phase [5] as well as in solution [5–7], liquid [5,6,8–10] and crystalline [5,6,8] forms and later using matrix isolation techniques [11,12]. The spectral interpretation has been supported by theoretical studies in many cases [5,7,9–13]. The picture that emerges is that MCA adopts four possible geometries by rotation about the single bond within the methyl ester fragment ($H_3CO$-C=O) and that controlling the orientation of the cyano moiety (O=C-

$CH_2CN$). In the case of the first, the methyl group can be oriented *syn* or *anti* relative to the carbonyl group but the *syn* form is predicted to be considerably more stable by ~45 kJ $mol^{-1}$ (HF/6-31G*) [10] and thus the dominant arrangement for the methyl ester moiety. For the second, previous studies largely point to the cyano fragment being *syn* or *gauche* relative to the carbonyl group [5–12]. Theoretically, the energy difference between the two conformers involving the (O=C-C-C) dihedral angle (assuming a s*yn* arrangement within the methyl ester fragment based on its high stability described above) is predicted to be quite small (for example: 0.174 kJ $mol^{-1}$ [11], 0.94 kJ $mol^{-1}$ [10], 2.51 kJ $mol^{-1}$ [9]) and to favour the *syn* orientation over *gauche* [5,7,9–12]. This energy ordering guided the interpretation of the aforementioned IR and Raman results which identified characteristic spectral features of only the *syn* form or to a mixture of the *syn*/*gauche* conformers depending on the sample phase and temperature. With higher level calculations (B3LYP/6-31++G(d,p)), however, the *gauche* form does not correspond to an energy minimum. Instead, the cyano group is predicted to lie *syn* or *anti* to the carbonyl group with the *anti* form being more stable by 1.10 kJ $mol^{-1}$ [13]. With experimental and theoretical results in support of a (O=C-C-C) dihedral angle between 110$^o$ [9] and 180$^o$ [13] (with most ~140$^o$-145$^o$ [5,10,11]) forming a conformer that may or may not be more stable than the *syn* form (0$^o$) of MCA, additional investigation is clearly warranted. Rotationally-resolved spectra, having an intrinsic dependence on geometry, is well-suited for this task.

In this article, we report the first rotational spectroscopic study of the ground state of MCA. Coupled with high level quantum chemical calculations including both B3LYP-D3(BJ) and MP2 calculations with the aug-cc-pVTZ basis set, we unambiguously

determined that the lowest energy conformer in the gas phase adopts a geometry that is *syn* with respect to the arrangement of the C-O-C=O fragment and *near anti* about the C-C-C=O dihedral angle. The spectral assignment was confirmed by analysis of the characteristic $^{14}N$ quadrupole hyperfine splitting patterns which closely match theoretical estimates. The relative energy ordering of the four conformers of MCA is explained using natural bond orbital (NBO) and non-covalent interaction (NCI) calculations and the absence of spectral features due to higher energy forms is rationalized based on the derived potential energy surface. Resolution of the A/E splittings permitted derivation of the three-fold barrier of the methyl internal rotor which is in good agreement with theoretical estimates and with the results of related molecules. With the most stable form unambiguously confirmed, this study forms the basis for a future identification of MCA in the ISM.

*Computational Methods*

MCA has two rotatable bonds which are described by the dihedral angles θ and ϕ indicated in Figure 1. A two-dimensional potential energy surface (PES) was derived using the Gaussian 16 revision C.01 program [14] at the B3LYP-D3(BJ)/cc-pVTZ level of theory through a series of single point calculations, avoiding *a priori* assumptions regarding symmetry, by varying θ from -180° to 180° and changing the angle ϕ from 0° to 360° in 10° increments each. For each point, all other parameters were relaxed and the resulting surface is given in Figure 1. As expected, four conformers of MCA were identified from this PES including two low energy forms with $\theta = 0^o$ resulting in the O-$CH_3$ bond oriented *syn* to the carbonyl group and two much higher energy geometries in which θ =

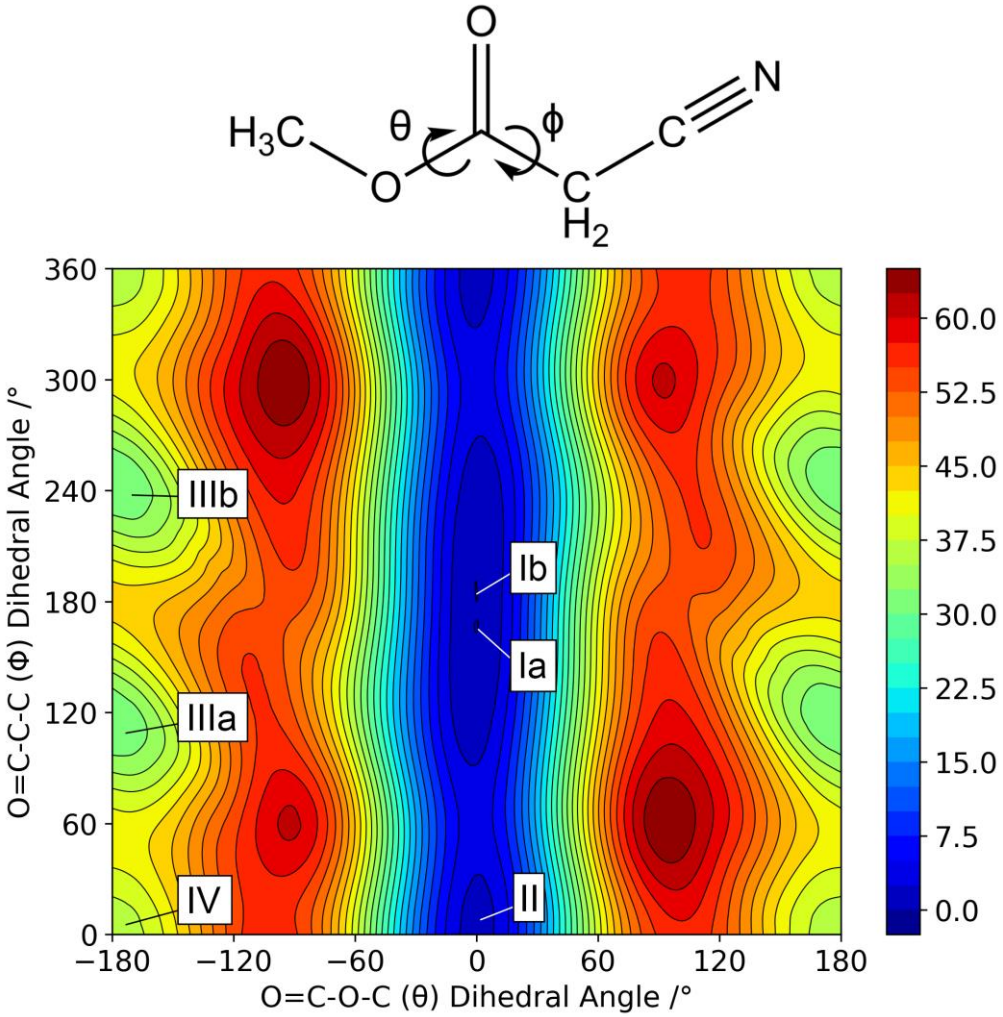


**Figure 1.** Potential energy surface of MCA calculated at the B3LYP-D3(BJ)/cc-pVTZ level of theory as a function of dihedral angles θ and ϕ defined above. The colour gradient represents the relative energy in kJ $mol^{-1}$. Minima correspond to four unique conformers with the enantiomer pair Ia/Ib defined as the global minimum geometry. Note that due to symmetry, the plot is mirrored through a point in the center.

180° (*anti*). The geometries of these four conformers were fully optimized at the B3LYP-D3(BJ)/aug-cc-pVTZ and MP2/aug-cc-pVTZ levels of theory and confirmed to be true minima based on their harmonic frequencies at the same level of theory. The optimized structures are displayed in Figure 2. The calculated rotational constants (A, B and C), $^{14}N$ nuclear quadrupole coupling constants (χ), electric dipole moment components ($\mu_a$, $\mu_b$,

$\mu_c$) and zero point corrected relative energies for each conformer of MCA are given in Tables 1 (DFT) and S1 (MP2).

Additional scans were conducted using both B3LYP-D3(BJ) and MP2 methods with the aug-cc-pVTZ basis set in order to understand the relaxation pathway of conformer II to conformer I by changing the angle ϕ in 20 increments of 10° while the

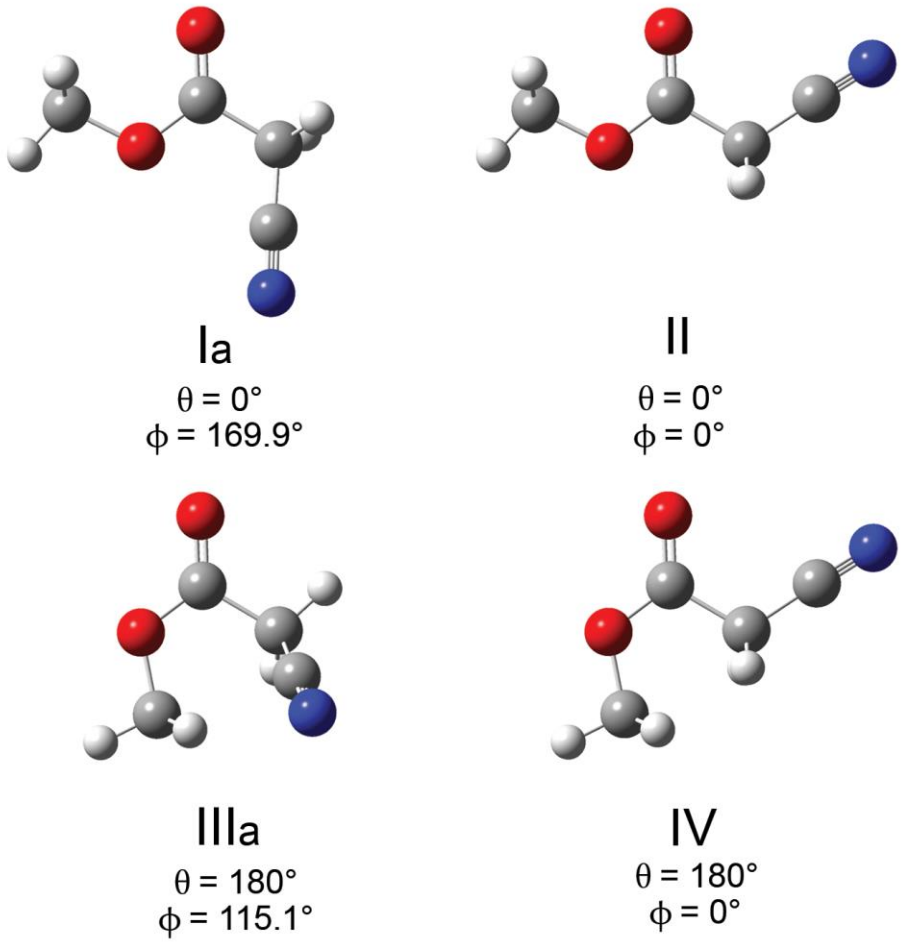


**Figure 2.** Geometries of MCA optimized at the B3LYP-D3(BJ)/aug-cc-pVTZ level of theory. Conformers I and III both have a mirror image where ϕ = 190.1° for Ib and ϕ = 244.9° for IIIb.

**Table 1.** Calculated spectroscopic parameters for the conformers of MCA obtained at the B3LYP-D3(BJ)/aug-cc-pVTZ level of theory.

| | Conformer Ia/b | Conformer II | Conformer IIIa/b | Conformer IV |
|---|---|---|---|---|
| A /MHz | 5068 | 9525 | 3770 | 6225 |
| B | 1839 | 1406 | 2265 | 1626 |
| C | 1376 | 1244 | 1595 | 1310 |
| $1.5\chi_{aa}$ /MHz | -2.041 | -5.096 | -3.572 | -6.955 |
| $0.25(\chi_{bb}-\chi_{cc})$ | -0.689 | -0.303 | 0.304 | -0.025 |
| $\lvert\mu_a\rvert$ /Debye | 2.34 | 4.62 | 0.21 | 4.86 |
| $\lvert\mu_b\rvert$ | 0.60 | 3.12 | 2.06 | 4.80 |
| $\lvert\mu_c\rvert$ | 0.45 | 0.00 | 3.33 | 0.00 |
| Energy[a]/kJ mol$^{-1}$ | 0 | 1.4 | 29.8 | 34.8 |
| Population[b] | 63.9% | 36.1% | 0.0% | 0.0% |

[a]Relative zero point energy corrected. [b]Boltzmann population at 298 K.

remaining parameters were allowed to relax. The barrier for the internal methyl rotation for conformer I was determined in a similar fashion by changing the value of θ in steps of 10°. The results of these scans are plotted in Figures 3 and 4, respectively.

To visualize the intramolecular interactions that govern the two most stable conformers of MCA, a non-covalent interaction (NCI) analysis [15] was carried out on the optimized geometries of I and II using the NCIPLOT [16] program. We also performed natural bond orbital (NBO) [17] calculations, including deletion of all antibonding and Rydberg-type orbitals, for all conformers of MCA at the B3LYP-D3(BJ)/aug-cc-pVTZ level to obtain the second-order perturbation energies corresponding to different charge transfer interactions and to decompose the full electronic energy into its Lewis (steric/electrostatic interactions) and non-Lewis (hyperconjugation) contributions. The NBO calculations were computed using the NBO 7.0 program. [18]

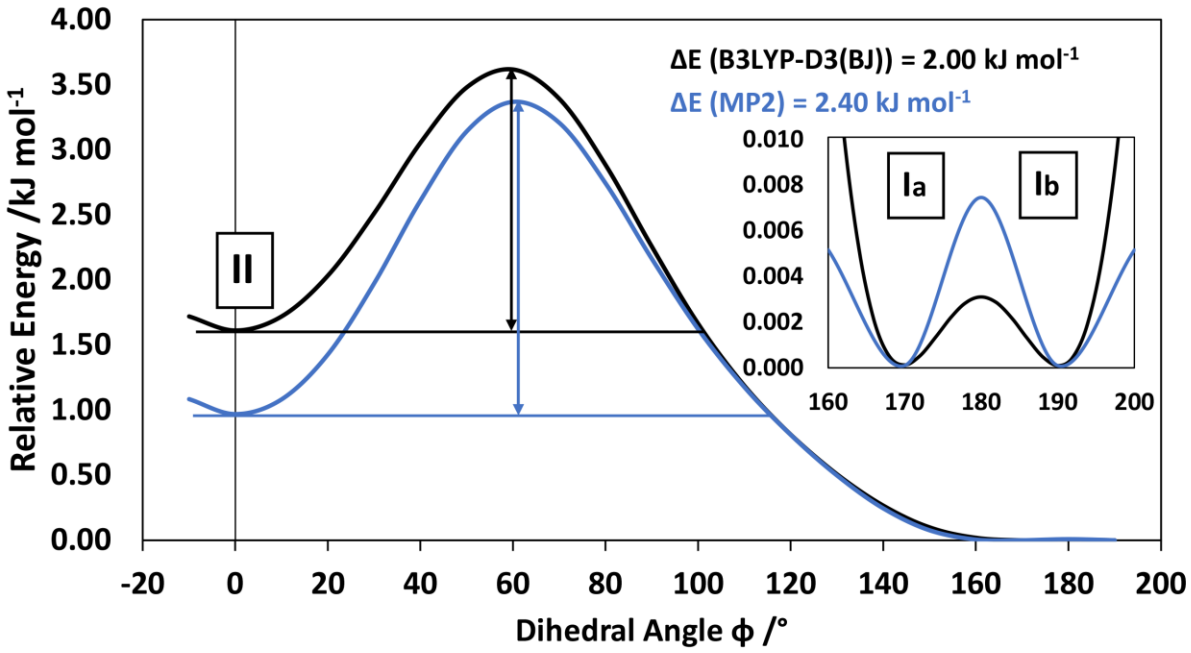


**Figure 3.** Potential energy curve for the interconversion of conformers I and II of MCA calculated at the B3LYP-D3(BJ)/aug-cc-pVTZ (black) and MP2/aug-cc-pVTZ (blue) levels of theory. The inset shows the details around minima at 169.9° and 190.1°corresponding to conformers Ia and Ib.

*Experimental*

A commercial sample of MCA (99%) was purchased from Alfa Aesar and used without further purification. Although liquid at room temperature (m.p. -23°C), MCA is not particularly volatile (b.p. 204°C) and consequently, ~ 2 mL of sample was placed into a stainless steel reservoir (½" internal diameter) seated in a band heater and mounted in the vacuum chamber ~ 10 cm upstream from a General Valve Series 9 pulsed nozzle with a 1 mm diameter orifice. The sample container was heated to ~ 80°C in order to coax the liquid into the vapour phase as neon (acting as an inert carrier gas) was passed over

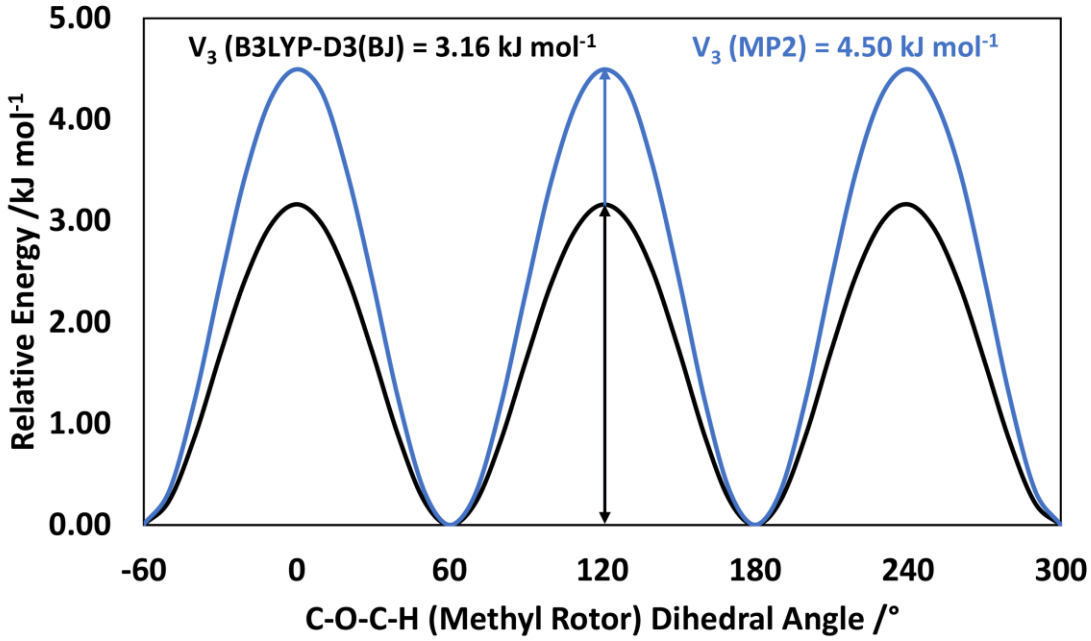


**Figure 4.** Potential energy curve for the methyl internal rotation of conformer I calculated at the B3LYP-D3(BJ)/aug-cc-pVTZ (black) and MP2/aug-cc-pVTZ (blue) levels of theory, where 0° is referenced to the H atom *antiperiplanar* to the carbonyl group.

it before supersonic expansion.

The rotational spectrum of MCA was collected from 6-19 GHz using chirped-pulse (cp) and Balle-Flygare (BF) Fourier transform microwave (FTMW) spectrometers which have been described previously [19,20]. The cp-FTMW spectrum was collected in 2 GHz segments in order to identify broad spectral patterns and make initial assignments. Higher resolution spectra were then collected with the BF-FTMW instrument in order to resolve splittings due to the $^{14}$N hyperfine structure as well as those due to the large amplitude motion of the methyl rotor. In a typical study with the BF-FTMW instrument, transitions can be measured with linewidths (FWHM) of 7 kHz and accuracy of ±2 kHz.

*Results*

From the relative energies derived in Tables 1 and S1, the vapour above a sample of MCA at room temperature should contain contributions from both conformers I and II while the higher energy forms (III and IV) have negligible concentrations. Conformer I is predicted to be more stable than II by 0.7 kJ $mol^{-1}$ (MP2) or 1.4 kJ $mol^{-1}$ (DFT) which corresponds to a relative Boltzmann population between 57% and 64% for the lower energy form at room temperature or slightly less (56% and 62%, respectively) at 80$^{o}$C (the temperature of the liquid sample) as the higher energy form is enriched. From the 2D PES in Figure 1, however, it should be noted that conformer I is actually an enantiomeric pair (Ia/Ib) in which the cyano moiety is rotated out of the plane of the ester fragment (-OC=O) by ±10.1$^{o}$ corresponding to the two minima at $\phi$ = 169.9$^{o}$ and 190.1$^{o}$ (when $\theta$ = 0$^{o}$). The conversion pathway between these two minima is plotted in the inset of Figure 3 and this process is essentially barrierless at both the MP2 and B3LYP-D3(BJ) levels of theory as the zero point energy will lie above the transition state at $\phi$ = 180$^{o}$. This implies that there is a large amplitude motion involving the $\phi$ dihedral angle. The presence of a double well potential for conformers Ia and Ib suggests that the gas phase composition of MCA could be further enriched in conformer I if one considers the populations of three states (Ia, Ib, II) but as the ground state of conformer I is above the barrier to Ia/Ib conversion, the composition of the MCA vapour before supersonic expansion is likely closer to the ranges predicted above.

Based on the estimated dipole components for conformer I of MCA in Table 1, the dominant form in the gas phase, the ground state rotational spectrum should exhibit

characteristic *a*-type patterns. Using the calculated spectroscopic constants (Table 1), the expected spectral features were simulated using the PGOPHER software [21] and the most intense lines in the cp-FTMW spectrum were readily assigned to conformer I. The veracity of the assignment was confirmed by the observation of less intense *b*-type transitions. Despite the presence of a $|\mu_c|$-dipole moment of 0.45 D, no *c*-type transitions were observed which is consistent with the barrierless interconversion between the minima corresponding to Ia and Ib on the PES that averages this dipole contribution to zero.

Subsequent higher resolution measurements using the BF-FMTW spectrometer revealed complex splitting patterns due both to the $^{14}$N hyperfine splitting as well as the A/E splitting of the methyl internal rotor. Figure 5 shows a sample spectrum for a strong *a*-type transition. The XIAM program [22] was used to fit the transitions in the A and E states simultaneously in order to obtain the experimental threefold barrier to internal rotation ($V_3$), the angle between the rotor α-axis and the principal inertial *a*-axis of the molecule (δ), the rotational constant of the methyl top ($F_0$), as well as the rotational, quartic centrifugal distortion and $^{14}$N quadrupole coupling constants. These are summarized in Table 2. The centrifugal distortion constant $D_K$ was not well-determined in the fit and hence was fixed to the theoretical value resulting in a fit of 153 lines with a rms standard deviation of 2.4 kHz.

In spite of the large dipole moments predicted for conformer II in Table 1, no transitions consistent with conformer II were observed. Given the high boiling point of MCA, the overall signal intensities (even with additional heating) were not sufficient to assign transitions due to minor isotopologues in natural abundance.

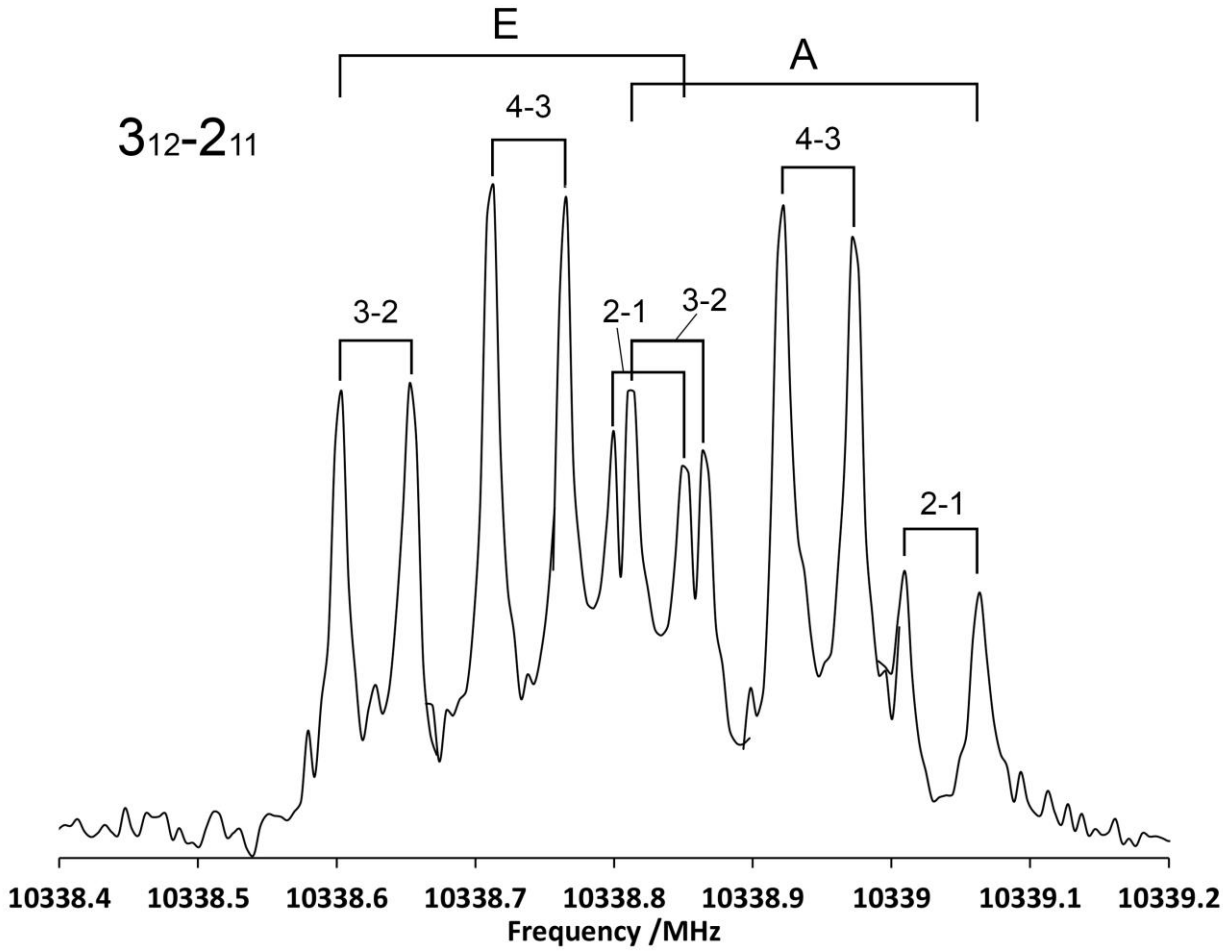


**Figure 5.** Sample Balle-Flygare spectrum detailing the splitting patterns due to the $^{14}N$ hyperfine structure and the internal rotation of the methyl group for a single rotational transition. The labels are for the F'—F" quadrupole hyperfine components. Note that this spectrum is composed of smaller segments collected with different excitation frequencies, each averaging 50 cycles.

**Table 2.** Spectroscopic parameters for conformer I of MCA.[a]

| | XIAM | B3LYP-D3(BJ)/aug-cc-pVTZ | MP2/aug-cc-pVTZ |
|---|---|---|---|
| A /MHz | 5069.2803(10) | 5068 | 5083 |
| B | 1842.95524(23) | 1839 | 1851 |
| C | 1383.81674(17) | 1376 | 1388 |
| $D_J$ /kHz | 0.5087(19) | 0.571 | 0.581 |
| $D_{JK}$ | 1.102(12) | 3.59 | 5.22 |
| $D_K$ | [2.07] | 2.07 | 0.247 |
| $d_1$ | -0.1769(20) | -0.234 | -0.230 |
| $d_2$ | -0.0458(14) | -0.118 | -0.151 |
| $1.5\chi_{aa}$ /MHz | -1.7886(24) | -2.041 | -1.678 |
| $0.25(\chi_{bb}-\chi_{cc})$ | -0.6912(12) | -0.796 | -0.649 |
| $V_3$ /kJ mol$^{-1}$ | 4.579(6) | 2.6255[c] | 4.50 |
| $F_0$ /GHz | 160.34(22) | 157.43 | 157.44 |
| δ /rad | 0.4829(7) | 0.4213 | 0.4150 |
| No. of lines | 153 | | |
| σ /kHz | 2.4 | | |

[a]Watson's S-reduced Hamiltonian ($I^r$ representation). [b]Root-mean-square deviation of the fit. Values in [ ] were fixed to the calculated values. [c]Zero point energy corrected.

*Discussion*

Based on the agreement of the experimentally-derived spectroscopic constants for MCA in Table 2 with the quantum chemical estimates, the observed rotational spectrum is clearly that of conformer I. It should be noted that the equilibrium geometry (corresponding to points Ia and Ib in Figure 1) differs in theory from that of the expected ground state structure which is affected by the large amplitude motion about ϕ. This is likely the origin of the discrepancies in some of the theoretical and experimental centrifugal distortion constants as the former are based on harmonic estimates and would not account for such a motion.

The planar moment $P_{cc}$ can provide some guidance regarding the relationship between the ground state and equilibrium geometries as the heavy atom backbone of MCA lies largely in the *ab*-inertial plane. Using the predicted rotational constants of

conformer II (Table 1), for example, $P_{cc}$ is 3.13 amu Å$^2$ which can be interpreted as arising from the hydrogens that are not in the *ab*-plane. In a study of the contributions of $CH_3$ and $CH_2$ groups to $P_{cc}$ for otherwise planar molecules, Bohn *et al.* [23] showed a relatively common value of 1.45-2.15 amu Å$^2$ for each methyl or methylene group in the molecule. Applying this empirical result to conformer II, we see that $P_{cc}$/n, where n is the number of these groups, is in fact 1.57 amu Å$^2$ which is in the range reported for several formates, 1.55-1.63 amu Å$^2$, the closest structural equivalent to MCA reported in this compilation [23]. For comparison, $P_{cc}$ is slightly larger, 3.66 amu Å$^2$, for conformer I of MCA based on the quantum chemical estimates suggesting only minor contributions to the second moment when the CN group is rotated out of the ester plane by ±10.1º. Counterintuitively, the experimental value of $P_{cc}$ for conformer I is actually larger, 4.36 amu Å$^2$, than the theoretical estimate suggesting that the ground state heavy atom backbone, which is an expectation value over the large amplitude motion in ϕ, is less planar as a result of these contributions. The flatness of the potential energy curve in ϕ around the global minima (Ia/Ib) helps to rationalize discrepancies in the literature as to whether this conformer of MCA was *gauche* or *anti* based on calculations using lower levels of theory and basis sets [5,7,9–13]. The near agreement of the experimental rotational constants with their theoretical counterparts and the larger than expected value of $P_{cc}$ in this work suggest that the effective ground state geometry of MCA conformer I is probably best characterized as having the cyano group oriented between the *gauche* and *anti* position relative to the carbonyl group but closer to the latter making it *near anti.*

The absence of transitions due to conformer II, despite its sizeable dipole moment, suggests that this form is not metastable in the supersonic jet. This can be attributed to

conformational cooling, a process that is known to occur when the interconversion barrier is less than ~5 kJ mol$^{-1}$ which is an empirical guideline based on previous rotational spectroscopic measurements of various molecular systems [24]. In MCA, we estimate that the barrier for conformer II of MCA to relax to the lowest energy form is only 2.00 kJ mol$^{-1}$ (B3LYP-D3(BJ)/aug-cc-pVTZ) in Figure 3 which supports the conjecture that the relaxation is facile. The observation of only conformer I unequivocally confirms that this is the lowest energy conformer of MCA and is supported by the accompanying quantum chemical results. This is in agreement with a prior B3LYP/6-31++G(d,p) calculation [13] and with the band profiles of the gas phase IR spectrum of MCA [5]. The IR and Raman spectra in condensed phases consistently showed that conformer II (*syn*) was the most abundant or the only form present depending on the sampling conditions [5–9]. While seemingly disparate with the present results, the dipole moment of conformer II (7.74 D) is more than double that of conformer I (3.39 D) suggesting an increased stability of the more polar *syn* form when entering a condensed phase. This has been demonstrated in the matrix isolation studies of MCA that studied conformational cooling as a function of deposition conditions [11,12].

The derived barrier to methyl internal rotation based on analysis of transitions within the A and E states of MCA is 4.579(6) kJ mol$^{-1}$ which fits within Kleiner's definition of an intermediate barrier [25]. The result aligns closely with calculations at the MP2/aug-cc-pVTZ level of theory (4.50 kJ mol$^{-1}$) and is larger than that from B3LYP-D3(BJ)/aug-cc-pVTZ. Experimentally, the $V_3$ barrier of MCA is ~10% smaller than that of methyl acetate ($V_3$ = 5.0500(7) kJ mol$^{-1}$ [1] for the ester methyl group), suggesting that the cyano fragment has a small influence on the electronic structure of MCA at the methyl

substitution site. To understand the origin of this effect and to rationalize the relative stabilities of the conformers of MCA, we turned to the results of NCI and NBO analyses.

The NCI isosurfaces shown in Figure 6 map the attractive and repulsive intramolecular interactions of conformers I and II. Comparison of the two show that while they present similar contacts between the hydrogens of the methyl group and the carbonyl oxygen as a consequence of the *syn* orientation within the methyl ester fragment, the *near anti* disposition of the cyano group in conformer I favours a long-range intramolecular contact between this group and the ester oxygen. This interaction is visualized in the NCI plot of I by the slightly blue tinge on the isosurface in Figure 6 between these groups. It is worth noting that this stabilizing effect is also accompanied by a repulsive component (red colour) associated with the formation of a 4-membered ring from the weak interaction. The balance between these favourable and unfavourable interactions,

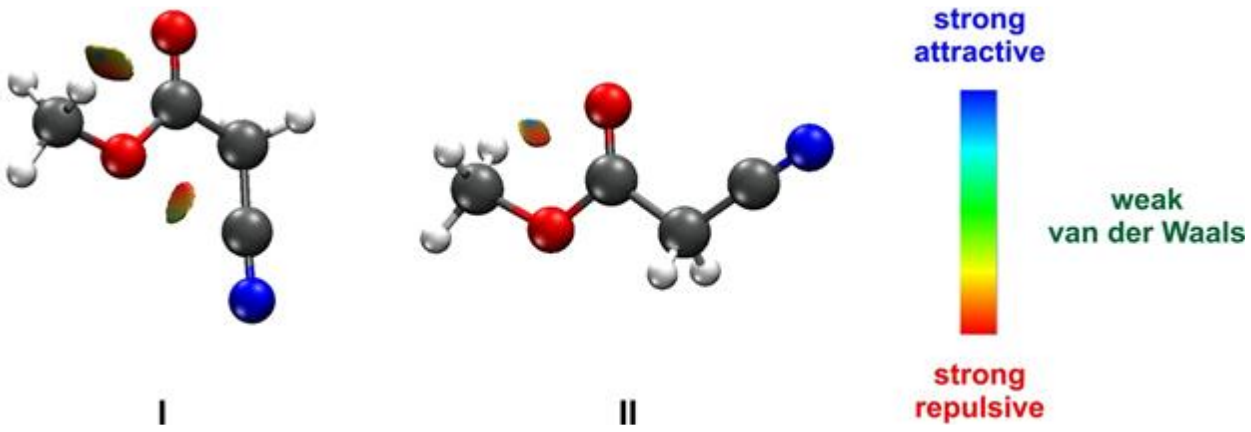


**Figure 6**. NCI isosurfaces (s = 0.05, colour scale of -0.02 < ρ < 0.02 au for the SCF densities) for the two most stable conformers of MCA.

embodied by the second isosurface for conformer I, is what ultimately governs the relative energies of conformers I and II.

To quantify the effects governing the stability of the conformers of MCA in detail, the full electronic energy of each conformer ($\Delta E_{total}$) was decomposed into its Lewis ($\Delta E_{Lewis}$) and non-Lewis ($\Delta E_{non\text{-}Lewis}$) type contributions using NBO calculations. These are summarized in Table 3. The $\Delta E_{Lewis}$ portion represents the overall steric/electrostatic effects present within each conformer while $\Delta E_{non\text{-}Lewis}$ is associated with stabilizing hyperconjugative orbital interactions. Previous work purports that conformers I and II (featuring a *syn* orientation of the methyl ester) are significantly more stable than III and IV (*anti* arrangement of the methyl ester) due to the antiparallel alignment of the C=O and C-O bonds [10,11]. The NBO results summarized in Table 3 reveal large values of $\Delta E_{Lewis}$ for conformers III and IV and thus provide an estimate of the magnitude of the destabilizing influences at work. From inspecting the geometries in Figure 2 and the nature of the occupied orbitals, it seems that the underlying cause of this significant destabilization of III and IV (relative to I and II) may very well be the near parallel orientation of the C=O and C-O bonds (as suggested earlier [10,11]) or may arise due to repulsion between the lone pairs on the ester oxygen and the carbonyl group.

Looking closer at the relative energy ordering of the pair of low lying conformers, the values in Table 3 reveal that while conformer I is more destabilized than II by steric interactions (reflected by the larger $\Delta E_{Lewis}$), it is also stabilized to a greater extent by favourable hyperconjugative interactions (as seen by the larger negative value of $\Delta E_{non\text{-}Lewis}$) when the cyano fragment is oriented *near anti* to the carbonyl group. The nature of these stabilizing influences can be deduced through comparison of the second order

perturbation corrections to the energies of conformers I and II from the NBO calculations. For example, the orbital interaction characterized as LP(O-ester)→π*(C≡N), which is only found in conformer I, stabilizes this geometry by 0.89 kJ mol$^{-1}$. Hyperconjugative effects involving the ester such as LP(O-ester)→π*(C=O) are found in both conformers I and II but contribute an extra 2.16 kJ mol$^{-1}$ to the former. This donation of additional electron density from the lone pairs on the ester oxygen to other regions of the molecule is consistent with the decreased $V_3$ barrier experimentally-derived in this work for MCA compared with that of methyl acetate [2].

**Table 3.** Relative energies of the Lewis ($\Delta E_{\text{Lewis}}$, steric/electrostatic) and non-Lewis ($\Delta E_{\text{non-Lewis}}$, hyperconjugative) interactions, in kJ mol$^{-1}$, for the four conformers of MCA obtained from the NBO calculations at the B3LYP-D3(BJ)/aug-cc-pVTZ level of theory.

| | $\Delta E_{\text{Lewis}}$ | $\Delta E_{\text{non-Lewis}}$ |
|---|---|---|
| I | 6.9 | -8.5 |
| II | 0.0 | 0.0 |
| III | 31.7 | -3.7 |
| IV | 35.0 | -1.2 |

*Conclusions*

Using a combined rotational spectroscopy and quantum chemical study, we have unequivocally shown that the lowest energy geometry of MCA is that in which the methyl and cyano fragments are positioned *syn* and *near anti*, respectively, to the carbonyl group (labelled as conformer I here). This settles a decades long discrepancy in the literature that pointed to a *syn*/*syn* arrangement (conformer II in this work) at the global minimum consistent with earlier theoretical reports [5,7,9–12]. The ground state geometry of

conformer I is highly averaged over a large amplitude motion involving the cyano fragment moving out of the plane of the ester backbone. The relative flatness of the potential energy surface with respect to the C-C-C=O dihedral angle has no doubt contributed to the challenges in establishing the nature of the global minimum on the PES of MCA. With the help of NBO calculations, we have identified that the slight balance in favour of conformer I over conformer II, which is found to be 0.7 kJ $mol^{-1}$ (MP2/aug-cc-pVTZ) or 1.4 kJ $mol^{-1}$ (B3LYP-D3(BJ)/aug-cc-VTZ) more stable, is due to increased hyperconjugative interactions such as LP(O-ester)→π*(C≡N) and LP(O-ester)→π*(C=O). The spectroscopic constants and methyl rotor barrier derived in this study lay important groundwork to investigate MCA in the millimeterwave region and may lead to its detection in astronomical sources.

*Acknowledgements*

This research is funded by the Natural Sciences and Engineering Research Council of Canada (NSERC) through the Discovery Grant program. CG is grateful for financial support provided through the SEGS program from the Faculty of Science at the University of Manitoba and WGDPS for support provided by a University of Manitoba Graduate Fellowship.

*Supplementary material*

Supplementary data to this article can be found online at https://doi.org/10.1016/.....

*References*

[1] B. Tercero, I. Kleiner, J. Cernicharo, H.V.L. Nguyen, A. López, G.M.M. Caro, Discovery of methyl acetate and gauche ethyl formate in Orion, Astrophys. J. Lett. 770 (2013) 1–6. https://doi.org/10.1088/2041-8205/770/1/L13.

[2] H.V.L. Nguyen, I. Kleiner, S.T. Shipman, Y. Mae, K. Hirose, S. Hatanaka, K. Kobayashi, Extension of the measurement, assignment, and fit of the rotational spectrum of the two-top molecule methyl acetate, J. Mol. Spectrosc. 299 (2014) 17–21. https://doi.org/10.1016/j.jms.2014.03.012.

[3] A. Das, L. Majumdar, D. Sahu, P. Gorai, B. Sivaraman, S.K. Chakrabarti, Methyl acetate and its singly deuterated isotopomers in the interstellar medium, Astrophys. J. 808 (2015) 14pp. https://doi.org/10.1088/0004-637X/808/1/21.

[4] H.S.P. Müller, F. Schlöder, J. Stutzki, G. Winnewisser, The Cologne Database for Molecular Spectroscopy, CDMS: A useful tool for astronomers and spectroscopists, J. Mol. Struct. 742 (2005) 215–227. https://doi.org/10.1016/j.molstruc.2005.01.027.

[5] S.J. Leibowitz, J. Laane, C. Van Alsenoy, B.J. van der Veken, On the Conformational Analysis of Methyl Cyanoacetate, J. Mol. Struct. 248 (1991) 251–273. https://doi.org/10.1515/zna-1977-0719.

[6] S.W. Charles, G.I.L. Jones, N.L. Owen, Vibrational spectra and rotational isomerism of methyl and ethyl cyanoacetate, J. Chem. Soc. Faraday Trans. 2. 69 (1973) 1454–1464. https://doi.org/10.1016/0022-2860(80)80364-4.

[7] R. Prasad, Y. Mishra, R. Gupta, Spectroscopic and molecular mechanics study of the conformational properties of methyl cyanoacetate and ethyl cyanoacetate, Indian J. Chem. -Section A. 29 (1990) 618–623.

[8] D. Sinha, J.E. Katon, The Vibrational Spectra of Methyl Cyanoacetate and Methyl Cyanoacetate- d 3 , Can. J. Chem. 52 (1974) 3057–3062. https://doi.org/10.1139/v74-448.

[9] C. Maury, J. Petrissans, Analyse structurale des dérivés fonctionnels des acides carboxyliques Partie II. Halogèno et cyanoacétates de méthyle, J. Mol. Struct. 246 (1991) 267–278. https://doi.org/10.1016/0022-2860(91)80133-O.

[10] J.M.F. Neta, R. Fausto, Molecular structure and vibrational spectra of methyl cyanoacetate: An FT-IR, raman and ab initio molecular orbital study, J. Mol. Struct. 443 (1998) 41–56. https://doi.org/10.1016/S0022-2860(97)00361-X.

[11] I.D. Reva, S. V. Ilieva, R. Fausto, Conformational isomerism in methyl cyanoacetate: A combined matrix-isolation infrared spectroscopy and molecular orbital study, Phys. Chem. Chem. Phys. 3 (2001) 4235–4241. https://doi.org/10.1039/b104671n.

[12] I.D. Reva, S.G. Stepanian, L. Adamowicz, R. Fausto, Missing conformers. Comparative study of conformational cooling in cyanoacetic acid and methyl cyanoacetate isolated in low temperature inert gas matrixes, Chem. Phys. Lett. 374 (2003) 631–638. https://doi.org/10.1016/S0009-2614(03)00782-6.

[13] A.D. Popova, Y.I. Binev, P.J. Vassileva-Boyadjieva, I.G. Binev, Experimental IR, and computational ab initio and DFT B3LYP studies on spectral and structural

changes, caused by the conversion of methyl cyanoacetate into carbanion, Bulg. Chem. Commun. 40 (2008) 512–519.

[14] M.J. Frisch, G.W. Trucks, H.B. Schlegel, G.E. Scuseria, M.A. Robb, J.R. Cheeseman, G. Scalmani, V. Barone, G.A. Petersson, H. Nakatsuji, X. Li, M. Caricato, A. V. Marenich, J. Bloino, B.G. Janesko, R. Gomperts, B. Mennucci, H.P. Hratchian, J. V. Ortiz, A.F. Izmaylov, J.L. Sonnenberg, D. Williams-Young, F. Ding, F. Lipparini, F. Egidi, J. Goings, B. Peng, A. Petrone, T. Henderson, D. Ranasinghe, V.G. Zakrzewski, J. Gao, N. Rega, G. Zheng, W. Liang, M. Hada, M. Ehara, K. Toyota, R. Fukuda, J. Hasegawa, M. Ishida, T. Nakajima, Y. Honda, O. Kitao, H. Nakai, T. Vreven, K. Throssell, J. Montgomery, J. A., J.E. Peralta, F. Ogliaro, M.J.. Bearpark, J.J. Heyd, E.N. Brothers, K.N. Kudin, V.N. Staroverov, T.A. Keith, R. Kobayashi, J. Normand, K. Raghavachari, A.P. Rendell, J.C. Burant, S.S. Iyengar, J. Tomasi, M. Cossi, J.M. Millam, M. Klene, C. Adamo, R. Cammi, J.W. Ochterski, R.L. Martin, K. Morokuma, O. Farkas, J.B. Foresman, D.J. Fox, Gaussian 16 Revision C.01, (2016).

[15] E.R. Johnson, S. Keinan, P. Mori-Sánchez, J. Contreras-García, A.J. Cohen, W. Yang, Revealing Noncovalent Interactions, J. Am. Chem. Soc. 132 (2010) 6498–6506. https://doi.org/10.1021/ja100936w.

[16] J. Contreras-García, E.R. Johnson, S. Keinan, R. Chaudret, J.-P. Piquemal, D.N. Beratan, W. Yang, NCIPLOT: A Program for Plotting Noncovalent Interaction Regions, J. Chem. Theory Comput. 7 (2011) 625–632. https://doi.org/10.1021/ct100641a.

[17] F. Weinhold, C.R. Landis, E.D. Glendening, What is NBO analysis and how is it useful?, Int. Rev. Phys. Chem. 35 (2016) 399–440. https://doi.org/10.1080/0144235X.2016.1192262.

[18] E.D. Glendening, J.K. Badenhoop, A.E. Reed, J.E. Carpenter, J.A. Bohmann, C.M. Morales, P. Karafiloglou, C.R. Landis, F. Weinhold, NBO 7.0, (2018).

[19] G. Sedo, J. van Wijngaarden, Fourier transform microwave spectra of a new isomer of OCS- $CO_2$, J. Chem. Phys. 131 (2009) 044303. https://doi.org/10.1063/1.3186756.

[20] L. Evangelisti, A. Grabowiecki, J. van Wijngaarden, Chirped pulse fourier transform microwave study of 2,2,2-trifluoroethyl formate, J. Phys. Chem. A. 115 (2011) 8488–8492. https://doi.org/10.1021/jp2047129.

[21] C.M. Western, PGOPHER: A program for simulating rotational, vibrational and electronic spectra, J. Quant. Spectrosc. Radiat. Transf. 186 (2017) 221–242. https://doi.org/10.1016/j.jqsrt.2016.04.010.

[22] H. Hartwig, H. Dreizler, The Microwave Spectrum of trans-2,3-Dimethyloxirane in Torsional Excited States, Zeitschrift Für Naturforsch. A. 51 (1996) 923–932. https://doi.org/10.1515/zna-1996-0807.

[23] R.K. Bohn, J.A. Montgomery, H.H. Michels, J.A. Fournier, Second moments and rotational spectroscopy, J. Mol. Spectrosc. 325 (2016) 42–49. https://doi.org/10.1016/j.jms.2016.06.001.

[24] R.S. Ruoff, T.D. Klots, T. Emilsson, H.S. Gutowsky, Relaxation of conformers and

isomers in seeded supersonic jets of inert gases, J. Chem. Phys. 93 (1990) 3142–3150. https://doi.org/10.1063/1.458848.

[25] I. Kleiner, Spectroscopy of Interstellar Internal Rotors: An Important Tool for Investigating Interstellar Chemistry, ACS Earth Sp. Chem. 3 (2019) 1812–1842. https://doi.org/10.1021/acsearthspacechem.9b00079.